MESOSCALE METEOROLOGICAL MODELING AT KILOMETER SCALE GRID MESHES FOR AIR QUALITY SIMULATIONS

Jason Ching*
*Institute for the Environment, The University of North Carolina, Chapel Hill, NC, USA

Rich Rotunno [1], Peggy Lemone [1], Alberto Martilli [2] Branko Kosovich[1], Pedro Jimenez [1], and Jimy Dudhia[1]
[1] NCAR, Boulder CO; [2] CIEMAT, Madrid Spain

1. INTRODUCTION

We address a basic issue associated with mesoscale WX models used for AQ models with fine [O(1km)] grid meshes. Such meshes are small enough to capture features of the larger turbulent eddies that may exist in the planetary boundary layer (PBL), but too large for the simulation of the turbulent cascade that regulates their amplitude and structure. Higher-resolution mesoscale modeling with current PBL parameterizations developed for the larger-grid-mesh simulations can simulate the often observed quasi two-dimensional convectively induced secondary circulation (CISCs) features occurring in the heated PBL (Figure 1) but performed without sound theoretical foundation, and thus are inaccurate and misleading (We call these simulated features, M-CISCs). In this and in Ching et al., 2013, we provide a theoretical explanation for M-CISCs. We also explore the using WRF-LES as a means for a more soundly based simulation of these ubiquitous CISCs and as a means for improving future mesoscale modeling parameterizations. We also explore alternative parameterization options that cause the model to reduce or restrict the generation of M-CISCs for more operational applications.

2. SITUATION

In recent years, as computers have become more powerful, high-resolution [O (1 km)] numerical simulations are being performed using mesoscale models like WRF to investigate dispersion of pollutants, urban meteorology, the impacts of land-surface heterogeneity, aspects of the boundary layer, the origin and evolution of convective precipitation, and hurricanes. Figure 2 shows how by reducing the grid mish size, the modeled features (here, the simulated mixing heights) become increasingly more spatially resolved. Convectively induced secondary circulations (CISCs), typically less than 10 km across, are a common feature of these simulations during unstable conditions. While mesoscale modeled-CISCs (M-CISCs) can look realistic, we raise several questions regarding their reality, origins, and impact. Figure 3 shows simulated vertical velocity at 125 m AGL at 2000 UTC (1400CST) for Houston Texas Area based on 1 km grid mesh for seven PBL schemes in WRF3.2 along with MODIS satellite cloud imagery for 1720 UTC. Assuming the cloud form in response to PBL circulations, the vertical velocity fields provide a crude surrogate for the cloud fields. We see that the WRF simulations produce horizontal patterns similar to the satellite fields but large and varied differences are seen in the patterns based merely on the PBL scheme.

A mesoscale model run at high resolution presents a major problem with respect to M-CISCs in that they are grid-size dependent with respect to amplitude, horizontal size and structure. In Ching et al., 2013 evidence is presented that this problem is one of the consequences of modeling flows at resolutions that are too high to justify the PBL schemes used and yet are too coarse for an explicit calculation of turbulent transfer, i.e., these high-resolution mesoscale models are firmly within Wyngaard's (2004) terra incognita (Figure 4). For some PBL schemes and for grid meshes in the ~1km range the wavelength and orientation of clouds produced by roll M-CISCS can be similar to those observed, and their vertical velocities are of the same order as observed. However, as the grid spacing becomes smaller, M-CISC patterns and their scale changes, and growth rates increase. M-CISCs locally modify virtual-temperature, mixing-ratio, and wind profiles in such a way that they share vertical transports with the PBL schemes.

**Corresponding author:* Jason Ching, Institute for the Environment, UNC-Chapel Hill, 659 Bank of America Plaza, CB#6116, Chapel Hill, NC 27599-6116; e-mail: jksching@gmail.com

3. Theory

For this study, we have used the classical linear theory (Rayleigh 1916) to show that M-CISCs are the result of instability due to PBL parameterization-produced superadiabatic lapse rates (Figure 5). We demonstrated this for both an idealized WRF simulation and a WRF simulation of an observed fair-weather boundary layer. In both cases, M-CISCs are generated after sufficient amount of surface heating occurs, the model simulated lapse rates become superadiabatic, causing the Rayleigh number to become supercritical. Subsequently, the M-CISCs thus generated, take over part of the vertical transport from the PBL scheme to make the virtual-temperature profile more neutral and after some time, the Rayleigh number becomes subcritical, which slows the growth down or ceases altogether. The theory thus explains why some PBL schemes (such as YSU and MYNN2) produce weaker CISCs (cf Figure 3), since their non-local transport terms make the potential temperature profile more nearly neutral and thus keeps the Rayleigh number near or below its critical value. Figure 6 shows the evolution of simulated soundings for a TKE based PBL scheme (MYJ), and one where a non-local closure scheme has been added (YSU 3.2) for CASES-99 field observation site in the Midwest USA. Both simulate the classical superadiabatic lapse rates seen in the observations, but YSU produces a near neutral thermal stratification and much reduced M-CISCs compared to MYJ. The theory also predicts an increase in growth rate of superadiabatically induced perturbations with smaller grid spacing as shown in Figure 5 and demonstrated and shown in Figure 7 (e.g., MYJ).

4. LES

In contrast to mesoscale models, Large Eddy Simulations (LES) have demonstrated their capability to simulate both CISCs and their associated turbulence field. The first LES simulations of convective atmospheric boundary layers were carried out by Deardorff (1970), who was the first to use *h/L* to distinguish roll regimes from those with more random convective structure (Deardorff (1972). Moeng and Sullivan (1994) used LES to contrast the roll and more convective regimes in more detail. For our current study, we have performed several additional numerical experiments using WRF-LES to demonstrate how CISCs can be simulated in ideal cases for a variety of flow and stability conditions. We varied the surface sensible heat flux and geostrophic forcing, $U_{g,}$ to explore the combined effect of shear and buoyancy on the convective boundary layer structures. Results are shown in Figure 8, for $-h/L$ = 10 and $-h/L$ = 100. Clearly, roll-like and cellular-like features are simulated for these two different convective regimes. Moreover, for both situations, the convective heating produced the expected super-adiabatic near-surface temperature gradient (not shown). These results demonstrate the ability of one-way nesting and sufficiently large domains for LES to allow the natural development of CISCs. Thus, LES is promising candidate to providing a sound bases for developing and or testing advanced and improved PBL schemes applicable in terra incognita regimes.

5. Parameterizations approaches for M-CISCs

We further examined alternative methodologies to mitigate the uncertainties introduced in M-CISCs by current PBL schemes. Guided by the theory, we explored some modifications to the (Bougeault-Lacarerre (1989) PBL scheme to suppress the M-CISCs. The first approach fixes the turbulent Prandtl Number (so-called **PR3D**) so that the effective Rayleigh number remains subcritical (thus eliminating M-CSCs) while the second approach introduces non-local transport (**GAMMA**) to the heat-flux term to reduce the modeled superadiabatic lapse rates.

The results are compared to a standard WRF reference case and shown in Figure 9. The **PR3D** method successfully suppresses M-CISCs for horizontal grid spacing of 1 km, 500m and 250m. Thus the **PR3D** is capable of avoiding the formation of M-CISCs thus effectively parameterizing the effect of the instabilities induced by the superadiabaticity, in particular the vertical transport of heat. In this sense this is a truly RANS approach, since it is not based on the size of the structure and not limited by the numerical resolution; thus, it can be applied safely even in the terra incognita for applications in which M-CISCs can introduce unwanted structure. The disadvantage is that it removes real and observable CISCs, since it only parameterizes their effects. The modeling option towards suppressing M-CISCs has pros and cons and degrees of effectiveness. Consideration of whether the RANs (Reynold's Averaged Navier-Stokes) model equations are ensemble averaged or volume averaged is relevant to choice.

The **GAMMA** experiment succeeded in M-CISC suppression at 1 km though at the expense of introducing artificial stability in the upper convective boundary layer through the non-local term. Although **GAMMA** is a more physically

realistic parameterization of turbulent heat transfer, the results show that this approach continues to be dependent on grid size. The benefits and limitations of these and yet other alternative approaches will have to be revealed through further investigations

6. Summary and Discussion

This paper has emphasized practical and theoretical problems with the present-day simulations of M-CISCs. If future endeavors determine their impact on the resolved mean quantities to be of significance, then it is recommended that improved PBL schemes be developed and that such parameterizations account for the effects of CISCs and their interaction with smaller scales, following Wyngaard (2004).

Given the capabilities of LES, a reasonable approach would be to compare results of **PR3D**-, **GAMMA**- or similar simulations with LES-based statistics, to find the optimum approach to minimizing the differences. While beyond the scope of this study, this approach may provide a means for optimizing PBL formulations like **PR3D** and **GAMMA** for RANS modeling.

Regarding fine grid modeling applications in urban context, it might be noted that urban canopy options in WRF, allowing within canopy additional vertical layers, will likely influences potential temperature profiles (e.g., predicted superadiabaticity, and thus impact the simulated M-CISCs. This will be explored further.

However, despite the shortcomings identified herein, M-CISCs appear to improve forecasts of convective initiation as discussed by Kain et al. (2013) and mimic observed roll-CISCs such as those shown by Wakimoto and Wilson (1984) to interact with cells in a squall line to produce tornado- bearing thunderstorms. Further study is needed to identify the optimal combinations of resolution, PBL parameterization, and model diffusion for severe-weather forecast applications.

7. References

Ching, J, R. Rotunno, M. LeMone, A. Martilli, P.A. Jimenez, J. Dudhia, Convectively induced secondary circulations in fine-grid mesoscale numerical weather prediction models, Submitted to Monthly Wea Rev, Sep 27,2013.

Deardorff, James W., 1970: Preliminary results from numerical integrations of the unstable planetary boundary layer. *J. Atmos. Sci.*, **27**, 1209–1211. doi:

Deardorff, J. W., 1972: Numerical investigations of neutral and unstable planetary boundary layers. *J. Atmos. Sci.*, **29**, 91-115.

LeMone, M. A., 1973: The structure and dynamics of horizontal roll vortices in the planetary boundary layer. *J. Atmos Sci.,* 30,1077-1091.

LeMone, M. A., M. Tewari, F. Chen and J. Dudhia, 2013: Objectively determined fair-weather CBL depths in the ARW-WRF model and their comparison to CASES-97 observation. *Mon. Wea Rev.*, **141**, 30-54.

Moeng, C. -H., and P. P. Sullivan, 1994: A comparison of shear- and buoyancy-driven planetary boundary layer flows. *J. Atmos. Sci.*, **51**, 999-1022.

Rayleigh, L, 1916: On convection currents in a horizontal layer of fluid, when the higher temperature is on the under side, *Phil. Mag.*, **32**, 529–546.

Wyngaard, J. C, 2004: Towards numerical modeling in the “Terra Incognita”, *J Atmos. Sci.*, **61**, 1816-1826.

FIGURES

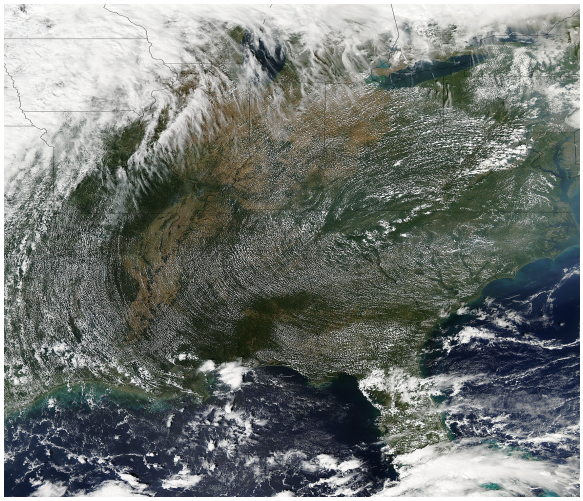

Fig. 1. Over land convectively-generated cloud fields in undisturbed flow conditions from MODIS satellite platforms. Image is approximately local noon. Data are from http://lance.nasa.gov/imagery/rapid-response.

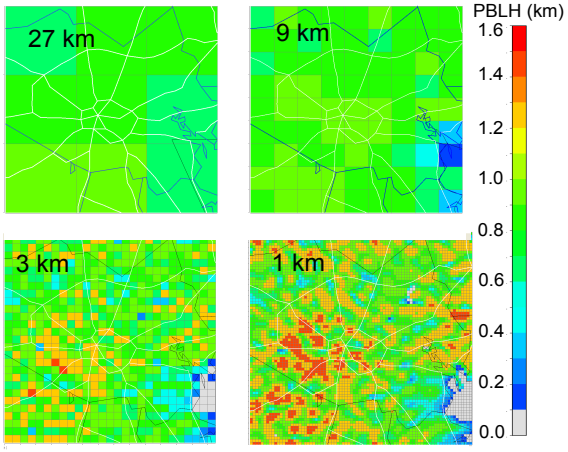

Figure 2. Nested WRF 3.2 model simulations of PBL height for 81 x 88-km model domain centered over Houston, TX for mid-day, August 4, 2006.

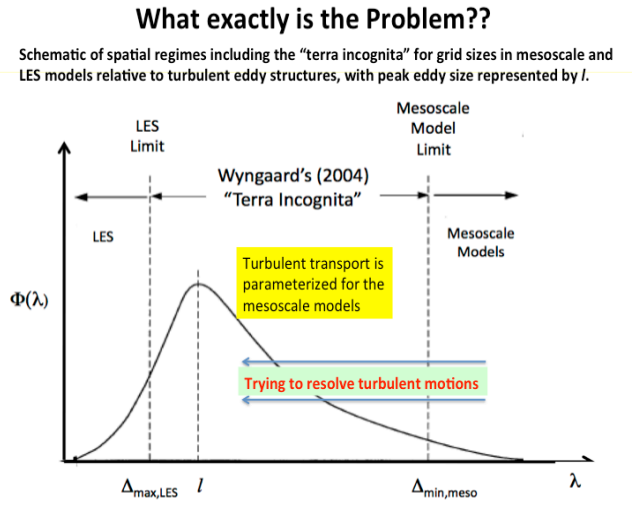

Fig. 4. Schematic showing the spatial regimes including the "terra incognita" for grid sizes in mesoscale and LES models relative to turbulent eddy structures, with peak eddy size represented by *l*.

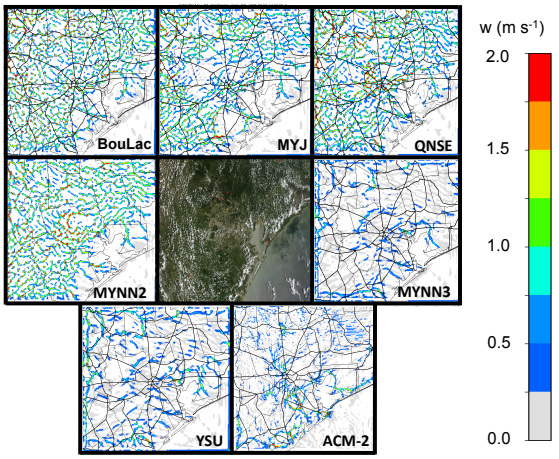

Fig 3. Comparison of observed PBL-generated clouds to results of positive vertical velocity at 125-m (Level 10) for 20 UTC August 4 over Houston-Galveston area using various PBL schemes in WRF. Satellite image, Terra 17:20 UTC, 500-m pixels: For the PBL schemes shown, vertical fluxes are proportional to local vertical gradients for BouLac, MYJ, QNSE, and MYNN2; while non-local vertical fluxes (independent of local vertical gradients) are also allowed for MYNN3, YSU, and ACM-2.

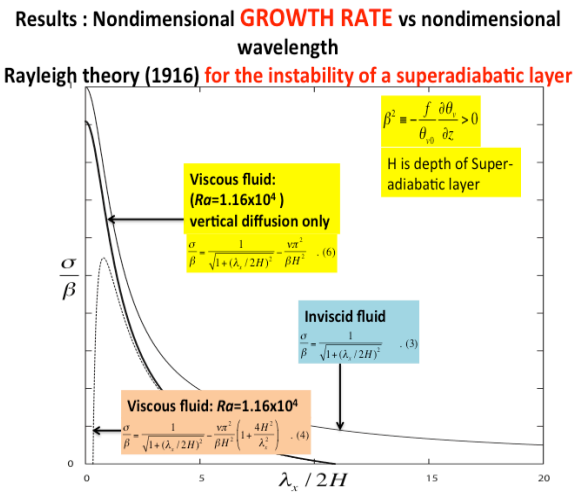

Fig. 5: Nondimensional growth rate versus nondimensional wavelength for the instability of a superadiabatic layer for inviscid, adiabatic flow (thin solid line), for viscous, adiabatic flow with $Ra = 1.16 \times 10^4$ (dotted line) and viscous, adiabatic flow with $Ra = 1.16 \times 10^4$, but with vertical diffusion only (thick solid line).

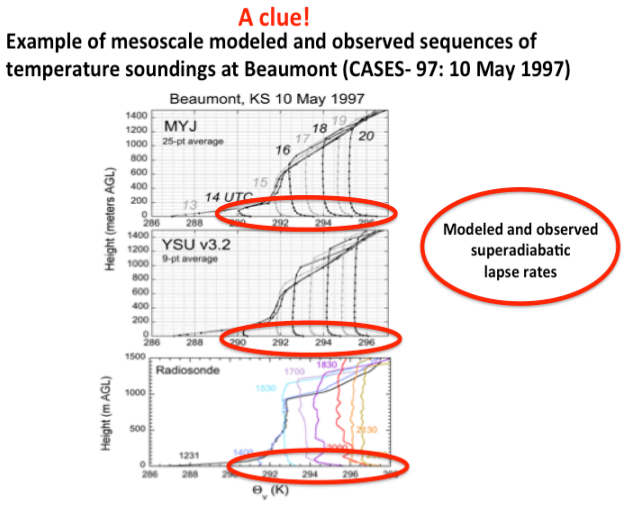

Fig. 6. For 10 May 1997, time sequence of Q_v profiles at Beaumont. Top, for MYJ, for horizontal average of 25 grid squares centered on Beaumont; middle, for YSU 3.2, for 9 grid squares centered on Beaumont; bottom, sequence of observed profiles

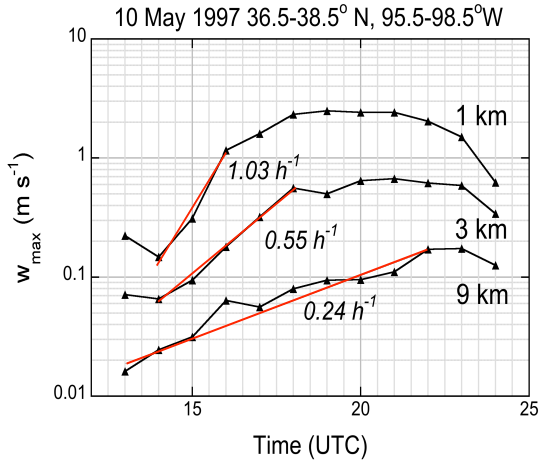

Fig. 7. For MYJ, maximum absolute value of *w* as a function of time for a domain centered over Beaumont, Kansas, for three simulations with Δ = 1, 3, and 9 km, no feedback from smaller scales. Least-squares best-fit lines correspond to the growth rates for each curve. Straight lines mark the time over which growth rate calculated.

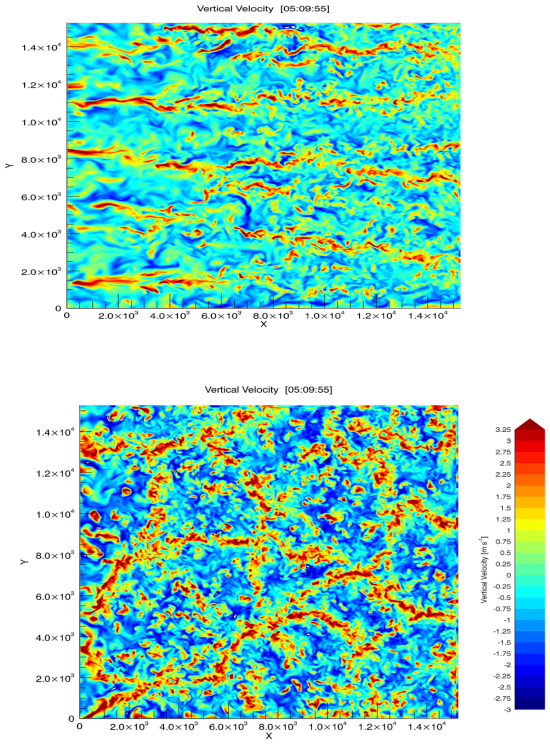

Fig. 8 (a) Contours of vertical velocity at a horizontal plane approximately 400m above the surface for LES of a convective boundary layer with - z_i/L=10 corresponding to a convective-roll regime. (b) Same as (a) except -z_i/L=100, the convective cellular BL regime. Note the scales are the same for both (a and b).

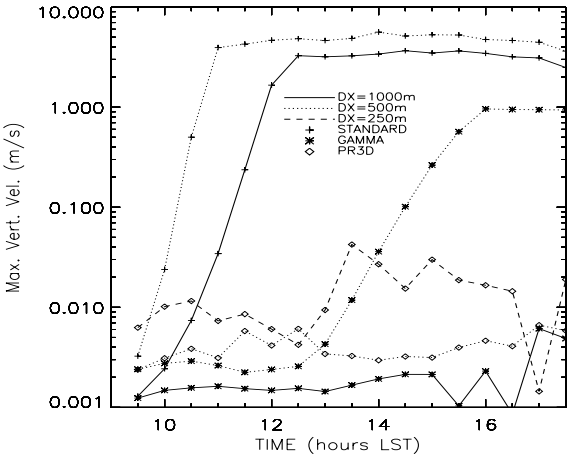

Fig. 9: Evolution in time of the maximum vertical velocity for the various simulations. The line type indicates the resolution, while symbols indicate the parameterization option.